

Architecture for image labelling in real conditions

Juan Manuel García Chamizo¹, Andrés Fuster Guilló¹, Jorge Azorín López¹

¹ U.S.I. Informática Industrial y Redes de Computadores. Dpto Tecnología Informática y Computación. Universidad de Alicante. Apdo. Correos 99. E-03080. Alicante. España
{juanma, fuster, jazorin}@dtic.ua.es <http://www.ua.es/i2rc>

Abstract. In this paper, an architecture for image segmentation and labelling obtained in real conditions is proposed. The model is based on the texture identification of the scene's objects by means of comparison with a database that stores series of each texture perceived with successive optic parameter values: collection of each perceived texture at successive distances, collection with successive light intensities, etc. As a basis for the architecture, self-organizing maps (SOM) have been used in several phases of the labelling process. The SOMs' discrimination capacity enables us to work on information extracted from the images, which has a low calculation cost. On the other hand, the reconfiguration possibilities of the neuronal network permit the systematic application of the proposed architecture, demonstrating the interest of its hardware implementation as a basis for an architecture with realistic vision. The article ends with an application of the architecture for labelling scenes in images when the distance at which the scene was captured is unknown.

1 Introduction

During the last few years, considerable advances have been made in vision techniques, however, there are still very few studies aimed at dealing with situations in natural environments, taking the scenes' realism into account; where natural light is changeable or isn't uniform; the scene's different planes become unfocused; the scale of an object's perception can change according to its distance; etc. [1], [2], [3]. The majority of studies have solved these problems with generally specific pre-processing methods, catalogued as enhancement or restoration methods [4], [5], [6].

When the aim is the segmentation and interpretation of the objects in a real scene, the task can be made easier if the configuration at surface texture level is known [7], [8], [9], [10]. Many techniques highlight the classification capacity of the characterizers extracted from images [11], [12] searching for properties that are invariable or tolerant with the variation of optic parameters [13], [14], [15], [16].

In the context of the research project *Vision system for autonomous navigation1*, one of the study's aims is the development of a light and realistic autonomous vision device. To this effect, this paper proposes a general segmentation and labelling model for real conditions acquired scenes, which could be systematically used in a wide

¹ This work was partly supported by the CICYT TAP1998-0333-C03-03

range of real situations (illumination, scale, focus variations...). The proposal tackles the problem by means of texture identification of the scene's objects, highlighting the simplicity of the characterizers used in the model, which will result in low computing costs and the possibility of formulating iterative algorithms aimed at solving real time problems.

Texture classification in real scenarios is carried out by consulting databases that store series of each surface captured with successive optical parameter values: the collection of each texture perceived at successive distances, the collection with different light intensities, etc. This approach implies the handling of large volumes of images. Consequently, the use of self-organizing maps [17], [18] to organize knowledge bases enables its discrimination capacity to be exploited and spatiotemporal costs to be reduced. On the other hand, the possibilities for hardware implementation of the self-organizing maps [19], will permit the model's systematic application by means of hardware reconfigurations

2 Problem Formulation

A given device, with a given calibration and in environmental conditions, has sensitivity around a value of the variable on which it operates, which is the so-called calibration point. The function that describes the device's behaviour acquires values at an interval around the calibration point. Generally speaking, we can assume that for another calibration point (and even for another device), the calibration function is different. For each device there will be a calibration point that generates an optimum calibration chart.

If Ψ is the value of an input magnitude to a sensor and, generally speaking, to a system, and $\Lambda^\alpha = \Lambda(x_j)$ is the function that represents the calibration to the values x_j of the n variables that characterize the sensor (environmental conditions or the system's characteristics). The sensor (system) output could be expressed as:

$$\alpha, \Psi f = f(\Psi, \Lambda^\alpha) \quad \forall^{\text{inf}} x_j \leq x_j \leq^{\text{sup}} x_j \quad j = 1 \dots n \quad (1)$$

For another calibration, the system output will be:

$$\beta, \Psi f = f(\Psi, \Lambda^\beta) \quad \forall^{\text{inf}} x_j \leq x_j \leq^{\text{sup}} x_j \quad j = 1 \dots n \quad (2)$$

With an input Ψ and the system output $\alpha, \Psi f$ for one of the calibrations known; the output $\beta, \Psi f$ for another calibration could be synthesized.

$$\beta, \Psi f = T^s(\Lambda^\beta, \alpha, \Psi f) \quad (3)$$

The interest of this research consists of proposing a general method that carries out transformation T^s , independently of the studied variables x_j of the calibration function $\Lambda(x_j)$. This approach enables us to achieve our aim of proposing a general architecture for image treatment. The arguments could reflect, for example, lighting conditions of the acquisition: with an image $\alpha, \Psi f$ captured with deficient lighting $\Lambda^\alpha = \Lambda(x_{\text{illumination}})$, the method will allow us to synthesized a new image $\beta, \Psi f$ with improved lighting conditions Λ^β . The same can be said for other variables, such as image resolution, which is the case in question in this paper.

Other transformation models could be dealt with, such as the estimate of the calibration function value Λ^β that generates the image ${}^{\beta,\Psi}f$ for an input Ψ , we will call T^Λ .

$$\Lambda^\beta = T^\Lambda \left({}^{\beta,\Psi}f \right) \quad (4)$$

Another transformation model T^Ψ of fundamental interest consists of obtaining the region labelling function ${}^\Psi\theta$ of the image ${}^{\beta,\Psi}f$, acquired with values of the calibration function Λ^β .

$${}^\Psi\theta = T^\Psi \left({}^{\beta,\Psi}f \right) \quad (5)$$

The region labelling function ${}^\Psi\theta$ must be independent of the calibration function values, that is, invariable to the context.

$${}^\Psi\theta = \theta(\Psi) = {}^\Psi\theta \left({}^{\beta,\Psi}f \right) = {}^\Psi\theta \left({}^{\alpha,\Psi}f \right) \quad (6)$$

In this paper, we will focus on the use of the transformations expressed in (4) and (5) to deal with the segmentation and labelling of a scene from an image.

3 Solution proposal

The formulation of the problem that has been carried out in the previous section is open and depending on the transformation functions characteristics T (3) (4) and (5) and on the knowledge we have of these functions, different methods can be proposed to solve the problem.

In the simplest cases, the result could be obtained analytically if the functional expressions for T are known. In the specific case of image treatment, as these functional expressions are not known, we will have to work in explicit terms resorting to databases that contain the magnitude values. To be more specific, this work is based on the use of textures. Labelling is obtained by comparing the descriptor of an unknown texture with the descriptors previously stored in a database for different materials and different calibrations. Consequently, the proposed general model of transformation T uses knowledge bases to infer the calibration function values Λ^α (4) or provide the region labelling function ${}^\Psi\theta$ (5). In any case, the inference from image ${}^{\beta,\Psi}f$, with the image ${}^{\alpha,\Psi}f$ being known for different calibration values Λ^α , is suggested. We will call these databases $DB({}^{\alpha,\Psi}f, \Lambda^\alpha)$. Consequently, we could formulate the expressions thus:

$$\Lambda^\beta = T_{DB}^\Lambda \left({}^{\beta,\Psi}f, DB({}^{\alpha,\Psi}f, \Lambda^\alpha) \right) \quad (7)$$

$${}^\Psi\theta = T_{DB}^\Psi \left({}^{\beta,\Psi}f, DB({}^{\alpha,\Psi}f, \Lambda^\alpha) \right) \quad (8)$$

The consultation of databases in (7) and (8) can be simplified by previously estimating the values Λ^α or Ψ and the subsequent consultation of the partial view of the databases for the known values of Λ^α or Ψ , we will call $DB_{\Lambda^\alpha}({}^{\alpha,\Psi}f, \Lambda^\alpha)$ or $DB_{\Psi}({}^{\alpha,\Psi}f, \Lambda^\alpha)$. In the proposal, the prior estimate of Λ^α is carried out for several reasons: we assume that the calibration function Λ^α values present a low spatial

dispersion with regard to the dispersion of the function $\Psi\theta$, on the other hand, the main aim of this study is to obtain region labelling and to a lesser extent, the estimate of the calibration parameters. Consequently, the calibration function Λ^α will be previously estimated by means of (7), which will enable us to obtain more precisely the region labelling function $\Psi\theta$ via consultation of the partial view of the databases $DB_{\Lambda^\alpha}(\alpha, \Psi f, \Lambda^\alpha)$ (9).

$$\Psi\theta = T_{DB, \Lambda}^\Psi(\beta, \Psi f, \Lambda^\beta, DB_{\Lambda^\alpha}(\alpha, \Psi f, \Lambda^\alpha)) \quad (9)$$

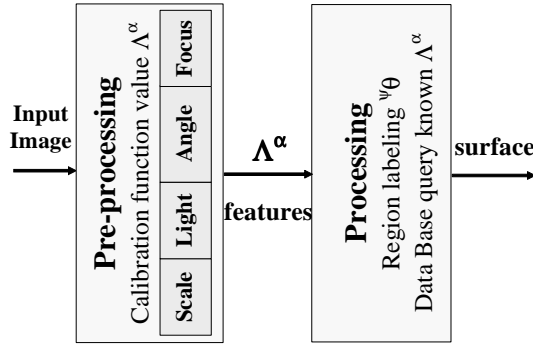


Fig. 1. Model for image labelling in real conditions

The steps are the following:

1. Pre-processing. Calibration estimation (7)

- Scan the unknown image with a window and classify each of the image's elements of the size of the window according to the best match found in the database, label the region with the calibration of the database element $DB_{\Lambda^\alpha}(\alpha, \Psi f, \Lambda^\alpha)$.
- Using the elemental calibrations, estimate the image calibration. Assumptions can be made on calibration uniformity in the whole image or in some parts. General calibration or calibration of the parts can be estimated as a statistical parameter of the elemental calibrations obtained for each position of the scan window. Other heuristics can also be used according to the knowledge and nature of the problem to be tackled; for example, the support of a complementary segmentation technique.

2. Processing. Image labelling (9)

Scan the unknown image again with a window and classify each image element of the window size according to the best match found in the view of the specific database for that calibration $DB_{\Lambda^\alpha}(\alpha, \Psi f, \Lambda^\alpha)$.

4 Architecture based on a reconfigurable SOM model

In order to tackle the scan windows' classification task of the unknown image by comparison with different images stored in databases, self-organizing maps have been used due to their discriminating capacity and high degree of parallelism inherent to connectionist methodologies. These self-organizing maps enable the discriminating

capacity of different features extracted from the images to be evaluated, that is, their suitability for grouping the unknown images together in accordance with different classification criteria, such as region labelling or the calibration value. On the other hand, these self-organizing maps will serve as the basis for a general architecture for the vision system in realistic conditions. The architecture will be general and will enable the problems of realism introduced by the different calibration variables to be dealt with by means of simple reconfigurations of the self-organizing maps neurons. To do this, we will use reconfigurable hardware, which has the ideal features for the proposed requirements, providing low level implementations with a high degree of parallelism and with reconfiguration capacity.

The self-organizing maps have been constructed from features extracted from the images $\tau^{(\alpha, \Psi)} f$ from the database $DB^{(\alpha, \Psi)} f, \Lambda^\alpha$ (different materials Ψ for different calibration function values Λ^α). According to the classification criterion for this set of features $\tau^{(\alpha, \Psi)} f$ different self-organizing maps are obtained; classified according to material $\Psi^\theta \text{SOM}(\tau^{(\alpha, \Psi)} f, \Lambda^\alpha)$ or to calibration function values $\Lambda^\alpha \text{SOM}(\tau^{(\alpha, \Psi)} f, \Lambda^\alpha)$.

The labelling of self-organizing maps per surface $\Psi^\theta \text{SOM}(\tau^{(\alpha, \Psi)} f, \Lambda^\alpha)$ may provide success levels that indicate the suitability, in certain cases, of the central part of processing to carry out region labelling Ψ^θ .

$$\Psi^\theta = T_{SOM}^\Psi \left(\beta, \Psi f, \Psi^\theta \text{SOM} \left(\tau^{(\alpha, \Psi)} f, \Lambda^\alpha \right) \right) \quad (10)$$

As we have previously mentioned, consultation of databases can be simplified by the prior estimation of the calibration values Λ^α and the subsequent consultation of the partial view of the databases $DB_{\Lambda^\alpha}^{(\alpha, \Psi)} f, \Lambda^\alpha$. These database partial views will be classified per material $\Psi^\theta \text{SOM}_{\Lambda^\alpha}(\tau^{(\alpha, \Psi)} f, \Lambda^\alpha)$. Once the calibration value Λ^β has been estimated, the map corresponding to this value is activated, as expressed in (11). These partial maps separated by calibration levels Λ^β do away with the overlapping of some patterns and thus offer better results.

$$\Psi^\theta = T_{SOM, \Lambda}^\Psi \left(\beta, \Psi f, \Lambda^\beta, \Psi^\theta \text{SOM}_{\Lambda^\alpha} \left(\tau^{(\alpha, \Psi)} f, \Lambda^\alpha \right) \right) \quad (11)$$

In the pre-processing phase, the calibration Λ^β , is also estimated by means of consulting the databases $DB^{(\alpha, \Psi)} f, \Lambda^\alpha$. We also use self-organizing maps labelled according to calibration values $\Lambda^\alpha \text{SOM}(\tau^{(\alpha, \Psi)} f, \Lambda^\alpha)$, as seen in (12).

$$\Lambda^\beta = T_{SOM}^\Lambda \left(\beta, \Psi f, \Lambda^\alpha \text{SOM} \left(\tau^{(\alpha, \Psi)} f, \Lambda^\alpha \right) \right) \quad (12)$$

As previously mentioned, database consultations can be simplified by prior estimation, in this case, of the values Ψ and the subsequent consultation of the partial view of the database for the known values of Ψ , we will call $DB_\Psi^{(\alpha, \Psi)} f, \Lambda^\alpha$. On the other hand, not all materials have the same suitability for calibration estimation, so, the complete database is used to carry out prior region labelling Ψ^θ (10), after which the surfaces suitable for estimating will be selected Λ^β . By separating the databases, in this case per surface, $DB_\Psi^{(\alpha, \Psi)} f, \Lambda^\alpha$, we can label the maps per calibration and select the ones that offer a higher degree of success (13).

$$\Lambda^\beta = T_{SOM, \Psi}^\Lambda \left(\beta, \Psi f, \Psi^\theta, \Lambda^\alpha \text{SOM}_\Psi \left(\tau^{(\alpha, \Psi)} f, \Lambda^\alpha \right) \right) \quad (13)$$

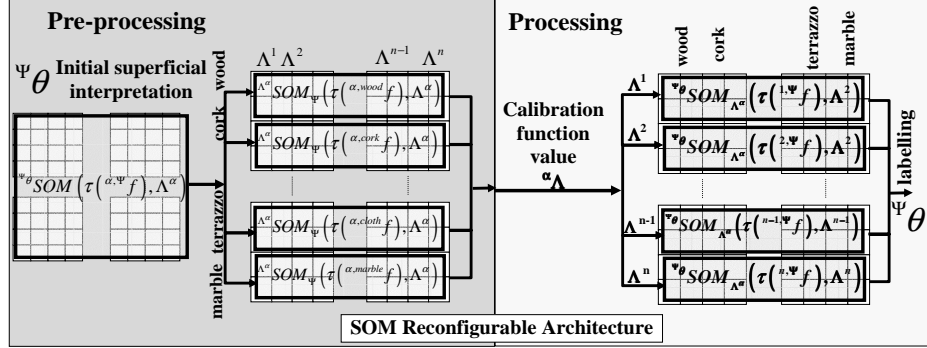


Fig. 2. The diagram shows the whole architecture for image labelling in real conditions based on reconfigurable SOMs

5. Architecture application in scale treatment

The model presented in the previous sections is general and could be used for the treatment of different calibration parameters such as lighting, scale, focusing conditions etc. In this section, its application will be specified on the analysis of the scaling level Λ^β .

An extensive collection of images capturing 14 materials (6 fabrics, 2 woods, marble, cork, 2 earthenware, terrazzo) with 150 scale values has been created, that is, 2100 captured images. In order to obtain these images, a programmable calibration capture system has been developed using a motorized optics Computar M10Z1118 and a high-resolution camera Hitachi KPF100 1300x1030. These collections have been obtained while maintaining a stable environment for the rest of the optical parameters. The numbers of pixels of each of the images, containing the materials, are dependent on the real world area in the scene. That is, the real world area captured for the construction of the database is the same for all the images, on all the scales, which means that more distant images have fewer pixels (86x86) than the nearest ones (783x783). After the previous cutting of the material surfaces of the 2100 images, these images have been cut into smaller samples of 80x80 pixels each, for reasons of coherence with the scan window size of the labelling algorithms. Number of samples ranges from 1 (the image with the least scale) to 81. Total samples is 29.890.

Table 1. Some of the samples of the database of different materials for different scale values

Scale (pix./cm)	fabric	cork	wood 1	wood 2	terrazzo	...
0 (2,81)					
149 (25,67)					

5.1 Self-organizing maps

The use of self-organizing maps has been proposed to classify features extracted from images in the database previously described. Below, we will describe the properties of each of the maps used in the process (characterizers used, number of neurons, success rates ...). We have previously mentioned that one of the model's advantages is the use of simple characterizers, which permit its iterative implementation as a basis for a generic architecture aimed at the tackling of problems with real time restrictions. The instances of the function $\tau^{(\alpha, \psi)} f$ have been different according to the labelling aims. For surface labelling of the functions (10) and (11), a generic characterizer such as the brightness histogram was used. With regard to scale value labelling (12) and (13), the characterizer used is the morphological coefficient histogram [20].

a) Classification rate of the self-organizing map to classify the complete database according to materials, expression (10): A classification rate of over 85% was obtained, that is, 85% of the patterns of the database (29.890) were correctly classified, the remaining 15% activated neurons linked to several materials. This enables us to approach region labelling, using exclusively this part of the process, in applications with relaxed requirements. The Number of neurones was 40 x 40.

b) Classification rates of the SOM for partial views of the database per scale values and labelling per surface, expression (11). The brightness histogram was used again for these databases. We observed improved results with regard to the classification of the complete database, as a result of dividing the problem. The 150 scale values are grouped into 15. The high scale values, from 9 to 14, were seen to offer slightly lower results as a result of insufficient areas of the materials being reflected.

Table 2. Classification rates of self-organizing maps for the expression (11)

Scale (pix./cm)	C. rate	Scale (pix./cm)	C. rate	Scale (pix./cm)	C. rate
0 (2,91)	100%	5 (5,18)	100%	10 (10,78)	96%
1 (3,18)	100%	6 (5,86)	100%	11 (12,88)	90%
2 (3,57)	100%	7 (6,75)	100%	12 (15,57)	95%
3 (4,03)	100%	8 (7,80)	100%	13 (18,95)	93%
4 (4,55)	100%	9 (9,11)	92%	14 (23,21)	87%

c) Classification rates of the SOM for the classification per scale value of the whole database (12): From the features studied, the best results regarding the labelling of this map correspond to the use of morphological coefficient histograms, although the total database doesn't offer sufficiently interesting results (20% classification rate). The characterizers studied, which are not specified in this paper, have sought the size of geometrical shapes in the materials' textures. The dimension of these shapes depends on the scale, as well as on the material studied, which makes scale classification difficult without prior knowledge of the nature of the material (12).

d) Classification rates of the self-organizing maps for the classification per scale value of the database separated according to surface (13): We found that the

separation of the database according to surface improved image classification with regard to scaling. Morphological coefficient histograms were also used for these maps. The classification rates of the SOM of the expression (13) grouped into 15 scale values, ranges from 68% of terrazzo to 48% of black wood. Assuming a low spatial dispersion of the scale in all the scene with regard to dispersion of the materials, the scale's general value could be estimated, as a statistical parameter of the elemental scale values obtained for each position of the scan window. The use of these maps in the more precise construction of scene depth maps requires the search for characterizers that provide better classification rates. These characterizers are not included in this study. However, as a low dispersion of scale in the scene is assumed, a high success rate, applying the mode as the statistical parameter, is obtained.

5.2 Scenario labelling

Once the classification capacities of the process's different maps have been reviewed, a series of tests with scenarios has been designed, based on the composition of real images not included in the database. Each of these scenarios contains the different surfaces corresponding to one of the scale values (from 2,91 pix/cm to 23,21 pix./cm).

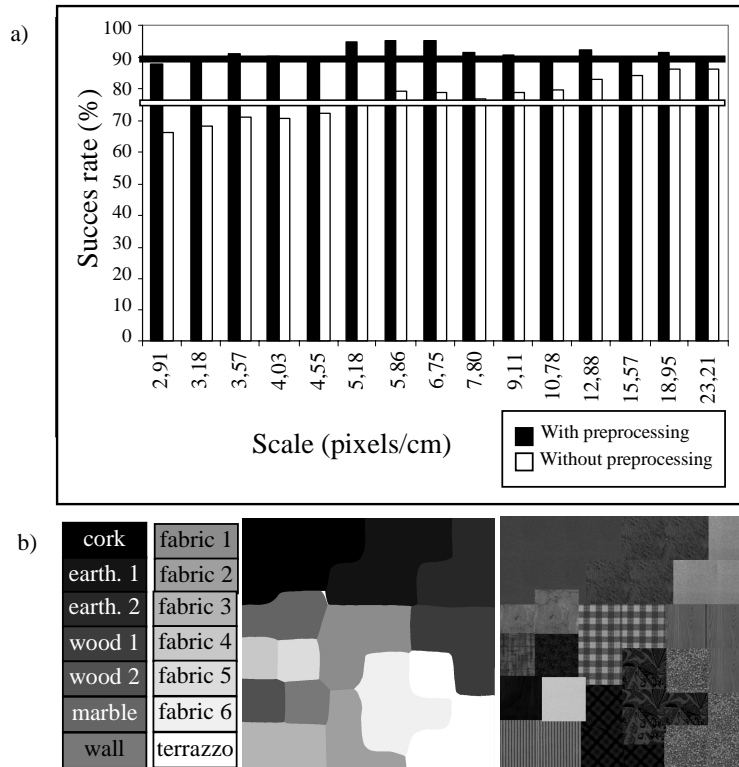


Fig. 3. a) In the following graph we can see the success rates of the use of the complete model as opposed to the model without pre-processing. b) One of the scenarios used as benchmark with its labelling results

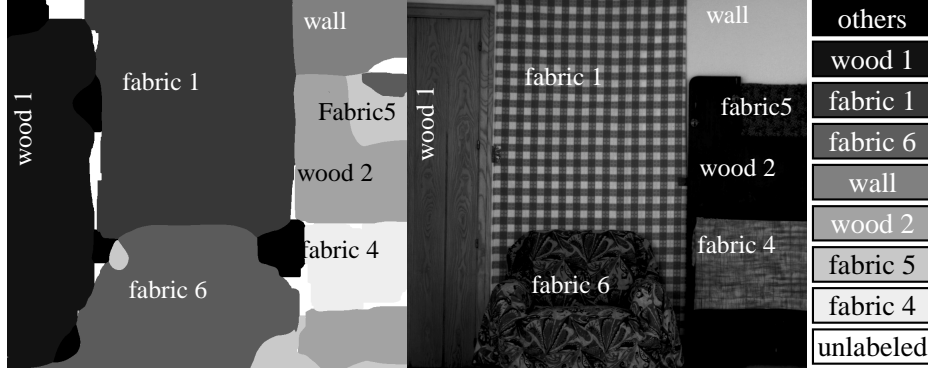


Fig. 4. We can see the good results (90,1 % of success rate) of the model's application in a real scenario with a scale value of 4,55 pixels/cm. The same scenario has been labelled without pre-processing obtaining a lower success rate (71,5 %) These results depend on the stability in the scene of the rest of the calibration variables not dealt with in the application.

6. Conclusions

This work offers an architecture for the segmentation and labelling of images acquired in realistic environmental conditions. The architecture has been conceived to systematically deal with the different causes that make vision difficult and allows it to be applied in a wide range of real situations: changes in lighting, changes in scale, faulty focusing, etc. The proposal is based on texture classification using self-organizing maps for the organization of databases that store series of each texture perceived with successive optical parameter values. More specifically, the results of the architecture applications in the labelling and segmentation of real scenes, perceived with different scale values, are reflected. The results show high success rates in the labelling of real scenes captured in different scale conditions, using very simple descriptors, such as different histograms of textures. This fact shows that self-organizing maps are suitable for solving this problem and can be used as a basis for a general, robust vision architecture. From the results obtained, our interest is directed towards systematizing the proposal and experimenting on the influence of the other variables of the vision process that have yet to be tested. Subsequently, we will propose an integral system for robust artificial vision that jointly considers all the parameters that can present difficulties for artificial visual perception. We will also tackle the implantation of the classifier module so that the different causes can be dealt with by the reconfiguration of the same hardware. To do this, we will use reconfigurable hardware, which has the ideal features for the proposed requirements, providing low level implementations with a high degree of parallelism and with reconfiguration capacity.

References

1. Jan Flusser and Tomáš Suk. Degraded Image Analysis: An Invariant Approach. IEEE Transactions on Pattern Analysis and Machine Intelligence, Vol. 20, No. 6, June 1998.
2. J. Biemond, R.L. Lagendijk, and R.M. Mersereau, "Iterative Methods for Image Deblurring," Proc. IEEE, vol. 78, pp. 856-883, 1990.
3. J.G. Moik. Digital Processing of remotely sensed images. NASA SP-431, Washington DC 1980
4. A Rosenfeld and AC Kak. Digital picture processing. Academic Press. New York, 2nd edition.
5. Rafael C. González, Richard E. Woods. Digital Image Processing. Addison-Wesley Publishing Company Inc. 1992.
6. M. Sonka, V. Hlavac y R. Boyle. Image Processing, Analysis, and Machine Vision (2nd edition). Brooks/Cole Publishing Company, 1998.
7. Chee Sun Won. Block-based unsupervised natural image segmentation. Optical Engineering, December 2000, Vol. 39(12).
8. Abhir Bhalerao y Roland Wilson. Unsupervised Image Segmentation Combining Region and Boundary Estimation. Image and Vision Computing, volume 19 (2001), number 6, pp. 353-368. August 2000.
9. N. W. Campbell, W. P. J. Mackeown, B. T Thomas, and T. Troscianko. Interpreting Image Databases by Region Classification. Pattern Recognition (Special Edition on Image Databases), 30(4):555--563, April 1997.
10. James G. Shanahan, James F. Baldwin, Barry T. Thomas, Trevor P. Martin, Neill W. Campbell, Majid Mirmehdi. Transitioning from Recognition to Understanding in Vision using Cartesian Granule Feature Models. Additive Proceedings of the Intn'l conference of the North American Fuzzy Information Processing Society, NAFIPS 1999, New York, pp 710-714. (Fritzke, 1997)
11. R.M. Haralick. Statistical and structural approaches to texture. Proceedings of IEEE. Vol 67. Pag 786-804. 1979.
12. H. Tamura, S. Mori and T.Yamawaki. Textural features corresponding to visual perception. IEEE Transactions on SMC. 8(6): 460 473, 1978.
13. F.S. Cohen, Z. Fan and M.A. Patel. Classification of rotated and scaled textured images using Gaussian Markov random field models. IEEE Transactions on PAMI. 13(2): 192-202,1991.
14. W.K. Leow and S.Y. Lai. Scale and orientation-invariant texture matching for image retrieval. Texture Analysis in Machine Vision. World Scientific 2000.
15. D.G. Sim, H.K. Kim and D.I. Oh. Translation, scale, and rotation invariant texture descriptor for texture-based image retrieval. Proceedings ICIP,2000.
16. A. Teuner, O.Pichler, J.O. Santos Conde, and B.J. Hosticka. Orientation-and scale-invariant recognition of textures in multi-object scenes. In Proc, ICIP, pages 174-177. 1997.
17. B. Fritzke. Some Competitive Learning Methods. Draft Paper, System Biophysics, Institute for Neural Computation, Ruhr-Universität Bochum, 1997.
18. T. Kohonen. Self-Organizing Maps. Springer-Verlag, Berlin Heidelberg, 1995.
- 19 D. Hammerstrom and N. Nguyen. An Implementation of Kohonen's Self-Organizing Map on the Adaptive Solutions Neurocomputer, in Artificial Neural Networks, T. Kohonen et al., (Eds.), Elsevier Science Publishers, 1991,pp. 715-719.
20. Juan Manuel García Chamizo, Francisco Ibarra Pico et al. Segmentation of defects in textile fabric using semi-cover vector and self-organization. Proceedings of the International Conference on Quality Control by Artificial Vision, France, 1995.